High-Resolution Ultrasound and MRI Imaging of Peroneal Tendon Injuries

5

L. Daniel Latt, Gokhan Kuyumcu, and Mihra S. Taljanovic

Introduction

Common disorders of the peroneal tendons include peroneal tendonitis, peroneal tendon tears, and peroneal subluxation or dislocation. While the presence of a peroneal tendon disorder is often suspected from the history and physical examination, advanced imaging is usually required to arrive at a precise diagnosis. Both MRI and US have been used in the evaluation of peroneal tendon disorders. There are advantages and disadvantages to each, although neither has demonstrated clear superiority. Ultrasound (US), with its dynamic imaging capabilities, is the study of choice in the evaluation of peroneal tendon instability, particularly transient intrasheath subluxation. Whereas, MRI is the better imaging modality to diagnose bone marrow edema like changes, as these cannot be detected on ultrasound.

A number of studies have evaluated the sensitivity and specificity of MRI in detecting tears of the peroneus brevis and longus tendons by comparison with intraoperative findings (Table 5.1). The majority of these have found MRI to be highly specific, but to lack some sensitivity in diagnosis of peroneal tendon tears. In contrast, studies comparing US to intraoperative findings have concluded that US is 100% sensitive, and more than 80% specific.

Our study of 21 patients with retromalleolar pain comparing US to MRI to intraoperative findings found that MRI identified 13/13 peroneus brevis tears, whereas

L. D. Latt (✉)
Department of Orthopaedic Surgery, University of Arizona College of Medicine, Tucson, AZ, USA
e-mail: dlatt@ortho.arizona.edu

G. Kuyumcu · M. S. Taljanovic
Department of Medical Imaging, University of Arizona College of Medicine, Tucson, AZ, USA
e-mail: mihrat@radiology.arizona.edu

M. Sobel (ed.), *The Peroneal Tendons*,
https://doi.org/10.1007/978-3-030-46646-6_5

Table 5.1 Results of studies comparing MRI and US to intraoperative findings

Modality	Study	Comparison	Peroneal tendon tear (sens/spec)	PB tear (sens/spec)	PL tear (sens/spec)
MRI	Lamm et al. [1]	Intraop. finding		83%/75%	50%/99%
	Khoury et al. [2]	Intraop. finding	91%/50%[a]		
	Park et al. [3]	Intraop. finding		44%/99%	50%/96%
US	Waitches et al. [4]	Intraop. finding (PL/PB/PT/ FDL)	100%/88%		
	Grant et al. [5]	Intraop. finding (PL/PB)	100%/85%		

[a]Values calculated from data presented in paper

Table 5.2 Results of unpublished study comparing MRI and US to intraoperative findings of peroneal tendinopathy, PB tear, PL tear, and subluxation in 21 patients with retromalleolar pain

	Tendinopathy	PB tear	PL tear	Subluxation
Intraoperative examination	18	16	4	3
MRI	18	16	4	1
US	18	14	4	3

US only found 11/13 (90% sensitivity); however, US detected 3/3 subluxating tendons whereas MRI only detected 1/3 (Table 5.2). In other words, MRI and US were both highly accurate in the detection of tears, but US was far more sensitive in detection of subluxation – a finding that was not discussed elsewhere in the literature.

To summarize, in the evaluation of peroneal tendon disorders, MRI has the advantage of supplying information about a wide array of related conditions that cause chronic lateral ankle pain including chronic ankle instability, osteochondral lesion of the talus (OLT), syndesmotic, and lateral ankle ligament injuries [6]. Moreover, MR images can be used by the orthopedic surgeon for operative planning. In comparison, US has the advantages of the following: (1) being a less expensive, shorter examination, (2) being capable of interactive dynamic examination which can be guided by the patient's symptoms such as the location of pain, or during provocative maneuvers, (3) allows for easy comparison with the contralateral side [7, 8], and (4) is more sensitive for detecting peroneal instability.

Imaging Techniques

Radiographs

The evaluation of all patients with chronic ankle pain should include weight-bearing three-view radiographs of the ankle (anteroposterior, lateral, and mortice). In the setting of retromalleolar pain, these radiographs are particularly useful for the following: (1) evaluating hindfoot alignment, (2) detecting avulsion fractures (Fig. 5.1), and (3) detecting a fracture of the os peroneum. Weight-bearing three views of foot

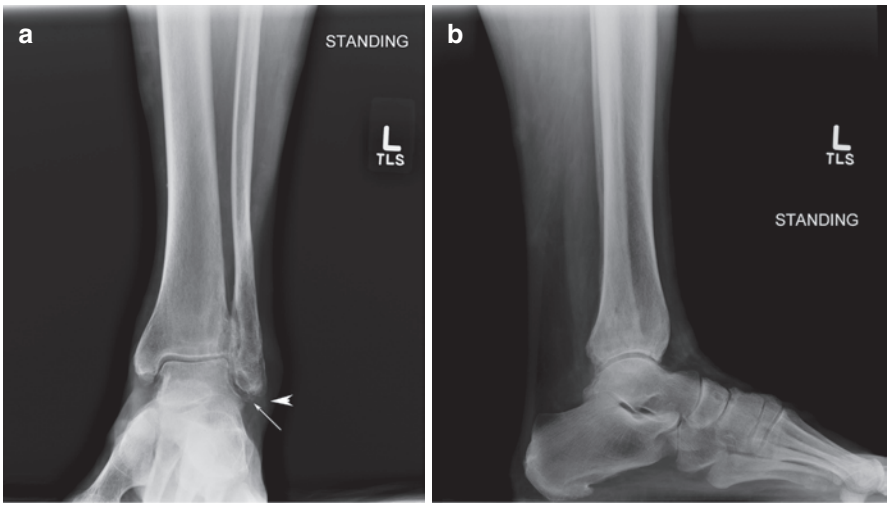

Fig. 5.1 Mortise (**a**) and lateral (**b**) standing radiographs of the left ankle. Mortise view shows soft tissue swelling overlying the lateral ankle (arrowhead) and small avulsion bone fragment (thin arrow) related to calcaneofibular ligament avulsion fracture

(anteroposterior, lateral, and oblique) should be obtained when varus or valgus hindfoot malalignment is suspected on clinical exam. Cavovarus malalignment (Fig. 5.2) causes lateral foot overload, is associated with peroneal tendon tears, and leads to protracted healing of lateral ankle ligaments and tendons. Cavovarus alignment is present in over 80% of patients undergoing surgery for peroneus longus tendon tears [9]. Similarly, planovalgus malalignment can cause narrowing of the inframalleolar space (subfibular impingement) leading to peroneal tendonitis and tendon tears. The standard weight-bearing radiographic views are usually sufficient, though a hindfoot alignment view [10] or long calcaneal alignment view may be useful to quantify the hindfoot varus.

MRI

Technique

MRI evaluation of the peroneal tendons is usually performed using a routine ankle protocol on a 1.5 T or 3.0 T machine [11, 12]. The ankle is placed in neutral inversion/eversion and approximately 20° of plantarflexion within a dedicated extremity coil (Fig. 5.3). The slight plantarflexion helps to separate the peroneal tendons within the common tendon sheath. Imaging sequences typically include both T1-weighted (anatomy) and T2-weighted or PD-weighted with fat saturation or STIR (fluid sensitive) in all three anatomic planes (axial, coronal, and sagittal relative to the distal tibia). The T1-weighted sequences are performed without fat saturation. A 3 mm slice thickness is used for all sequences except for sagittal STIR (4 mm slice thickness/0.5 mm gap). An additional three-dimensional gradient echo

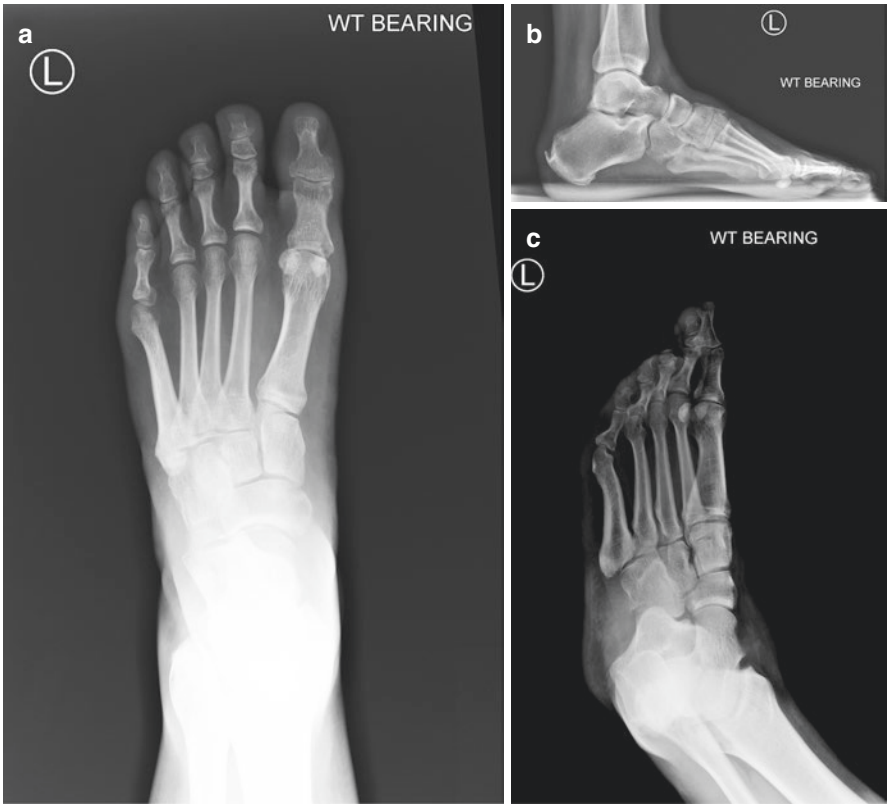

Fig. 5.2 Anteroposterior (**a**), lateral (**b**) and oblique (**c**) standing views of the left foot show cavovarus alignment of the left foot as evidenced by increased calcaneal pitch, sinus tarsi drive through sign, positive Meary's angle, and absent base of first and fifth metatarsal overlap on the lateral view as well as increase in parallelism between the talus and calcaneus and stacking of the tarsal bones on the anteroposterior view

sequence with submillimeter slice thickness (in our institution 0.7 mm) is often used to image the tibiotalar cartilage. Injuries to the peroneal tendons are usually well seen on the T1-weighted and fluid-sensitive sequences in three planes. However, injury to the distal portion of the PL on the plantar surface of the foot is sometimes better evaluated on additional sequences parallel and perpendicular to the long axis of the metatarsals.

Normal Findings and Pitfalls

Normal tendons have low signal intensity (black) on all MRI sequences (Fig. 5.4). Increased signal on all sequences indicates tendon disease that can be either tendinosis or tear. Fluid-sensitive sequences can help to identify the particular derangement. Signal heterogeneity and tendon thickening is typically associated with tendinosis while focal defects with associated increased signal are consistent with partial thickness tendon tears. Moreover, a collection of fluid around the tendon but within the sheath is characteristic of tenosynovitis. Signal heterogeneity and tendon

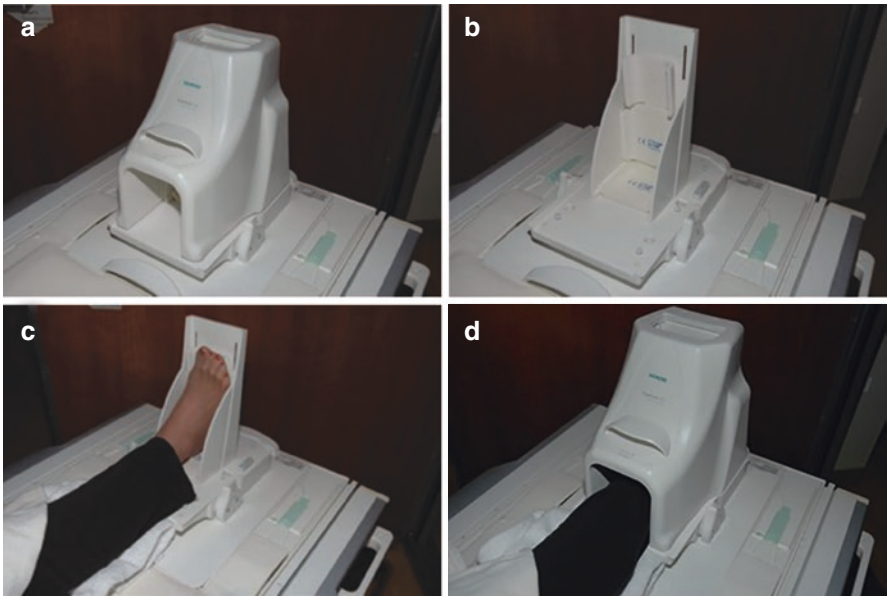

Fig. 5.3 Dedicated ankle extremity coil. The outer shell (**a**) and foot support (**b**) of a transmit–receive multichannel extremity coil for MRI. Ankle MRI is performed with the patient in the supine position and the ankle joint in the neutral position, with approximately 20° of plantar flexion (**c**). In the axial plane, the use of 20° of plantar flexion helps to separate the peroneal tendons in the common peroneal sheath. (**d**) The fully assembled ankle coil with patient in position

thickening is typically associated with tendinosis while focal defects with associated increased signal are consistent with partial thickness tendon tears. However, increased signal intensity can also be due to the magic angle effect whereby a structure oriented at 55° relative to the magnetic field has increased signal on T1-weighted (ET < 38 ms) sequences [13]. Plantarflexion of the ankle to 20° helps to minimize this effect. Furthermore, all findings made on T1-weighted sequences should be checked against the corresponding images on fluid-sensitive sequences to avoid misdiagnosis.

The configuration and shape of the tendons are also useful in determining the specific derangement. Within the retromalleolar groove, the normal PB has an oval, flat, or mildly crescentic appearance (fettuccini shaped) on axial sequences, whereas the PL has a more globular or circular cross-section (spaghetti shaped) [6, 12]. The slightly flattened cross-section of the PB should not be mistaken for a tear.

Ultrasound

Technique

In contrast to MRI in which routine imaging protocols are sufficient for the evaluation of the peroneal tendons, a specific protocol is required for the dynamic ultrasound evaluation of the peroneal tendons. The author's preferred technique is to use

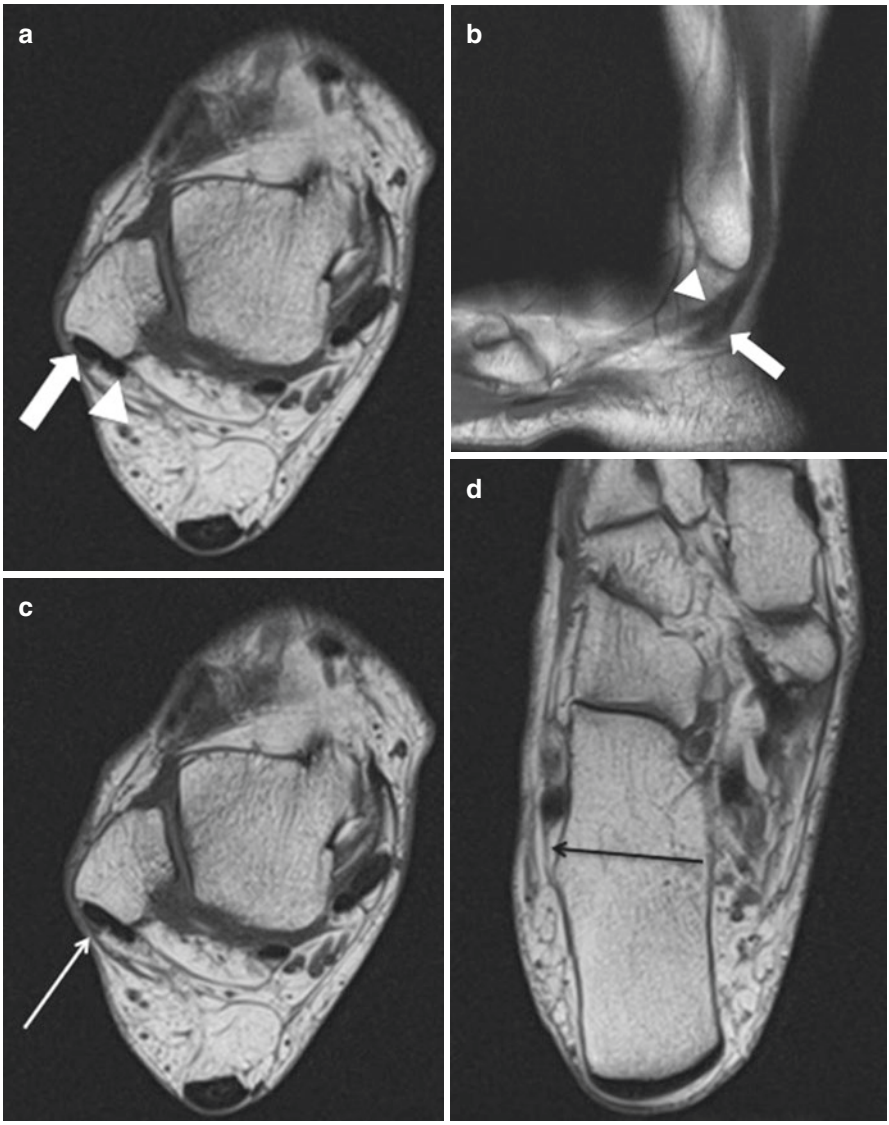

Fig. 5.4 Normal peroneal tendons, superior peroneal retinaculum (SPR) and inferior peroneal retinaculum (IPR): (**a**) Axial T1-weighted MR image shows the normal anatomy and positioning of the peroneal tendons. Peroneus longus (PL) tendon (white thick arrow) is situated anterior to the peroneus brevis (PB) tendon (white arrowhead) in the retromalleolar groove. The PB tendon is mildly flattened and crescentic and PL tendon is rounded. (**b**) T1-weighted sagittal MR image shows course of the PB tendon (white arrowhead) and attachment to the fifth metatarsal base. PL tendon course is also seen (white thick arrow). Note the homogenous hypointense signal throughout the PB and PL tendon course. (**c**) Axial T1-weighted MR image shows SPR (white thin arrow) overlying the peroneal tendons in the retromalleolar groove. (**d**) IPR (black thin arrow) is shown overlying both peroneal tendons at the hindfoot. (**e**) Axial T1-weighted MR image shows a normal concave retromalleolar groove (black arrow). (**f**) A shallow convex retromalleolar contour (white arrow) which is associated with an increased risk of peroneal tendon instability

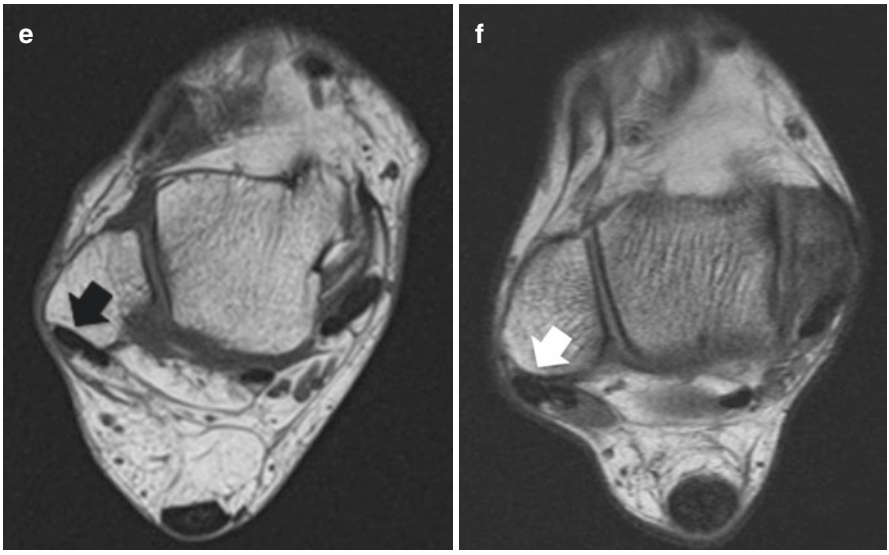

Fig. 5.4 (continued)

a high-resolution 8–18 MHz linear "hockey stick" probe with a small footprint. The patient is positioned in the supine position with the knee flexed approximately 45°–90° and the hip internally rotated to expose the lateral side of the ankle and foot. A large amount of gel is used especially around the curved surface of the lateral malleolus to avoid unnecessary pressure with the transducer which could displace the tendons. Imaging of the supramalleolar, retromalleolar, and inframalleolar portions of the PL and PB including the distal portion of their muscle bellies is performed in both the transverse (short-axis) and longitudinal (long-axis) planes. The examination begins proximally and proceeds distally. The tendons are imaged together until they take separate sheaths at the IPR, after which they are examined separately. The tendon sheaths are also examined for thickening, increased synovial fluid complexes, and hypervascularity using power Doppler or color Doppler imaging. The SPR is examined by orienting the transducer obliquely along its course. Dynamic examination of the SPR is performed to look for transient subluxation or dislocation of the peroneal tendons from within the sheath or intrasheath subluxation by having the patient perform resisted maximal dorsiflexion and eversion while the probe is oriented along the short axis of the tendons. The plantar portion of the PL is then imaged with the patient is prone position with the ankle plantar flexed to expose the plantar surface of the foot. The tendon is identified at its attachment at the base of the first metatarsal and followed on long and short axis views laterally and proximally until it reaches the cuboid tunnel.

Normal Findings and Pitfalls

The normal peroneal tendons appear hyperechoic and fibrillated on US [6, 7] (Fig. 5.5). They may appear hypoechoic due to anisotropy if the ultrasound transducer is not perpendicular to the examined tendon. This occurs commonly in the

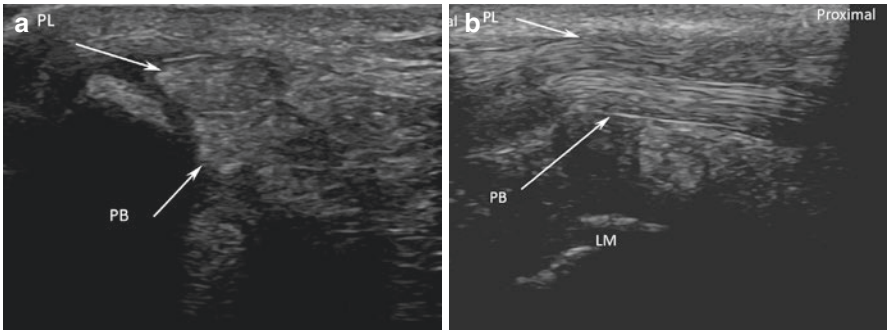

Fig. 5.5 US of normal peroneal tendons. Short-axis (**a**) and Long-axis (**b**) US images at the fibular retromalleolar groove show normal fibrillar texture and echogenicity of the PB and PL tendons

inframalleolar region where the probe must be tilted at the correct angle to follow each of the tendons [8]. The peroneal tendon sheaths are not normally seen on US unless they are distended by the presence of excess synovial fluid or synovial hypertrophy. The anterior portion of the SPR can be seen as a thin hyperechoic or hypoechoic band inserting onto the fibrocartilaginous ridge, whereas its posterior portion is difficult to visualize [7, 14]. The peroneal tubercle is seen protruding from the lateral aspect of the calcaneus with the overlying IPR which is often difficult to visualize. The os peroneum (when present) can be seen as a hyperechoic structure within the PL.

Functional Imaging

Shear wave elastography [15] is a recently developed technique which quantifies soft tissue stiffness (elasticity) in vivo and may eventually play a role in determining the prognosis for tendon and ligament disorders and thereby play a role in treatment decision making [16].

A shear wave is a secondary acoustic wave that is emitted by the linear US array prior to the imaging wave and is oriented perpendicular to the principal wave. The speed of propagation of the shear wave through the tissue is recorded. The shear modulus of the tissue can then be calculated from the shear velocity ($G = \text{rho} \times c^2$) if the tissue density is known [15].

Shear wave imaging is now FDA-approved on most state-of-the-art US scanners (including those offered by Philips, GE Healthcare, Siemens Healthineers, Ultrasonix, and Supersonic Imagine) for diagnostic imaging of the musculoskeletal system. Despite its use in research studies of a number of musculoskeletal tissues, including Achilles tendon, patellar tendon, and supraspinatus tendon, it has not gained wide clinical acceptance for musculoskeletal examination, as normative values and its role have not been defined. SWE of the chronically injured peroneal tendons might help determine which tendons are capable of healing and which require repair, tenodesis, or allograft reconstruction.

Peroneal Tendinosis, Tendonitis, and Tenosynovitis

Peroneal tendonitis (tenosynovitis) occurs commonly as a result of inversion ankle injuries and is often concurrent with ankle sprains, osteochondral lesions of the talus and other hindfoot derangements [17]. The tendon is injured by the forceful reflexive activation of the peroneal muscles to prevent the complete inversion of the foot. Tenosynovitis can also result from repetitive stress, rheumatologic diseases, or infection [6, 7, 12]. Patients often present with swelling and tenderness along the tendon sheath. On MRI, the tendons appear thickened with increased or heterogenous intensity signal (Fig. 5.6). The normal tendon sheath contains a small amount

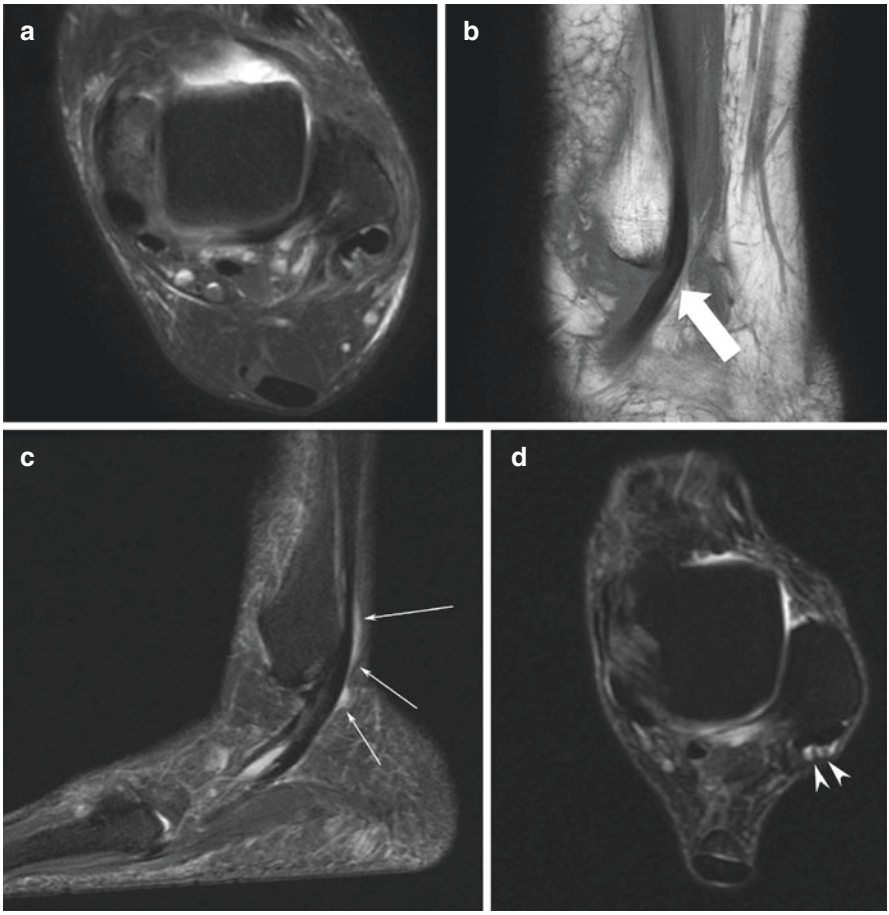

Fig. 5.6 Marked tendinosis of PB tendon without tear. (**a**) axial T2 Sagittal T1-weighted and (**b**) sagittal T1-axial T2-weighted fat-saturated MR images show marked thickening of the PB tendon (block arrow) without any tear or cleft consistent with tendinosis. Stenosing Tenosynovitis. (**c**) Sagittal STIR and (**d**) axial T2-weightedfat-saturated MR images show irregular distended peroneal tendon sheath with increased heterogeneous synovial fluid complex (thin arrows). In (**d**), note multiple linear low-signal-intensity bands (arrowheads) consistent with stenosing tenosynovitis

of tenosynovial fluid, up to 3 mm is considered normal [6, 18–20]. Edema may extend into the peritendious structures. The inflamed tenosynovium is best seen on fat-saturated contrast-enhanced T1 images. On US examination, the inflamed and thickened tendon, synovium, and peritendinous structures appear hypoechoic, whereas the synovial fluid appears anechoic. Power or color Doppler imaging can be used to show the increased vascularity of the inflamed synovium consistent with hyperemia.

In contrast, peroneal tendinosis is a noninflammatory degenerative process. It occurs in a number of settings that either decreases the space available for the peroneal tendons or chronically overloads the tendons. On MRI, the tendon appears thickened with increased signal intensity within the tendon substance on both T1 and T2 weighted sequences [6, 12, 18, 21, 22], whereas on US, the tendon appears hypoechoic and thickened, with no discrete tear [6] (Fig. 5.7). A decrease in the volume of the inframalleolar space can occur from subfibular impingement as in seen in patients with severe long-standing flatfoot when the lateral wall of the calcaneus comes to impinge on the distal fibula reducing the inframalleolar space available for the peroneal tendons. A relative decrease in the inframalleolar or retromalleolar space can be caused by a low-lying PB muscle belly or a peroneus quartus. Malunited calcaneus fracture also causes peroneal tendinosis as the blown out lateral wall decreases the retromalleolar and inframalleolar space. Chronic overload of the peroneal tendons can be caused by lateral ankle ligament instability, as the peroneal tendons must then assume the full role of stabilizing the ankle against inversion forces. This problem is commonly seen after an ankle sprain in patients with cavovarus alignment where the varus of the hindfoot puts all of the lateral ankle structures under constant load, including the peroneal tendons.

Stenosing tenosynovitis is a chronic condition which results from friction between the peroneal tendons and a narrowed inferior osseofibrous tunnel due to a hypertrophied peroneal tubercle and/or a thickened IPR [23, 24]. Long-standing compression of the tendons in the tunnel leads to tenosynovial fibrosis and synovial

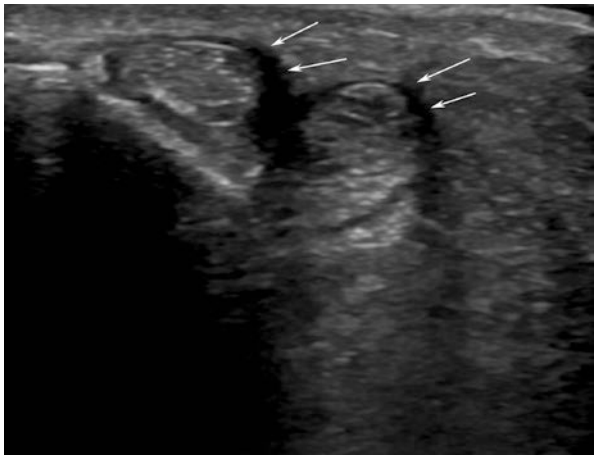

Fig. 5.7 Tendinosis and Tenosynovitis of PB and PL tendons. Short axis gray scale US image shows thickened heterogeneous peroneal tendons (thin white arrows) with increased surrounding hypoechoic synovial fluid complex in distended tendon sheath consistent with tendinosis and tenosynovitis

proliferation that limits tendon excursion. On MRI, the tendon fibrosis is seen as linear areas of intermediate or low signal intensity on all routine noncontrast sequences within the synovial fluid and tendon sheath which may contrast enhance. The absence of synovial fluid can be seen on the fluid-sensitive sequences [6, 12].

Peroneal Tendon Tears

Peroneal tendon tears should be suspected in any patient presenting with chronic lateral ankle pain located posterior or inferior to the tip of the lateral malleolus. They can occur as the result of either acute trauma (e.g., ankle sprain) or chronic degeneration. Tears are common (found in 11% of cadaveric specimens [25]), but fortunately, most are asymptomatic, thus they only require imaging investigation when symptoms persist after the acute injury has subsided. Tears usually occur as part of a complex injury (found in 30% of patients undergoing ankle instability surgery [26]) or in a malaligned hindfoot (cavovarus foot or planovalgus foot with subfibular impingement.

Peroneus brevis tears occur most commonly in the retromalleolar region where the PB is subjected to compression between the PL and the retromalleolar groove. There are a number of factors that predispose to tearing of the PB including the following: (1) shallow, convex, or irregular retromalleolar groove, (2) crowding due to low-lying PB muscle belly or (3) a peroneus quartus, and (4) subluxation or dislocation due to SPR tear [27]. In partial thickness tears, the PB is boomerang-shaped and envelops the PL, and this corresponds to the central thinning that occurs with tendon degeneration (Fig. 5.8). On MRI, the affected portion of the tendon has irregular intermediate signal intensity or hyperintensity. There is a corresponding hypoechoic internal echotexture with loss of normal fibrillation on US examination. Partial thickness longitudinal split tears are often associated with tendon thickening or thinning. In a thickened tendon, it is difficult to differentiate tendinopathy from partial thickness tear, whereas tendon thinning is almost always associated with partial thickness tearing [6, 7, 12].

Partial thickness longitudinal split tears usually involve the posterior portion of the PB. The fissuring of the tendon can progress anteriorly leading to a complete longitudinal split tear with the PL lying between two PB hemitendons (Fig. 5.9) [6, 7, 27]. The split tears always start in the retromalleolar region but may extend distally into the inframalleolar region where the tendon reconstitutes. On MRI, complete longitudinal split tears have a high or intermediate signal with discontinuity of the fibers [6, 12]. The hemitendons associated with these tears often have irregular borders. These tears are usually best visualized on axial and coronal MR images. On US, complete split tears appear hypoechoic or anechoic, with fluid at the tear site and discontinuity of the fibers. These tears can usually be seen on both short and long axis images at rest. Dynamic US examination in in ankle plantarflexion and subtalar eversion can help to bring out occult tears. Longitudinal split tears of the PB most often occur in conjunction with other lateral ankle soft tissue disorders including ATFL rupture (50%) and SPR tear. Complete tears (rupture) of the PB are

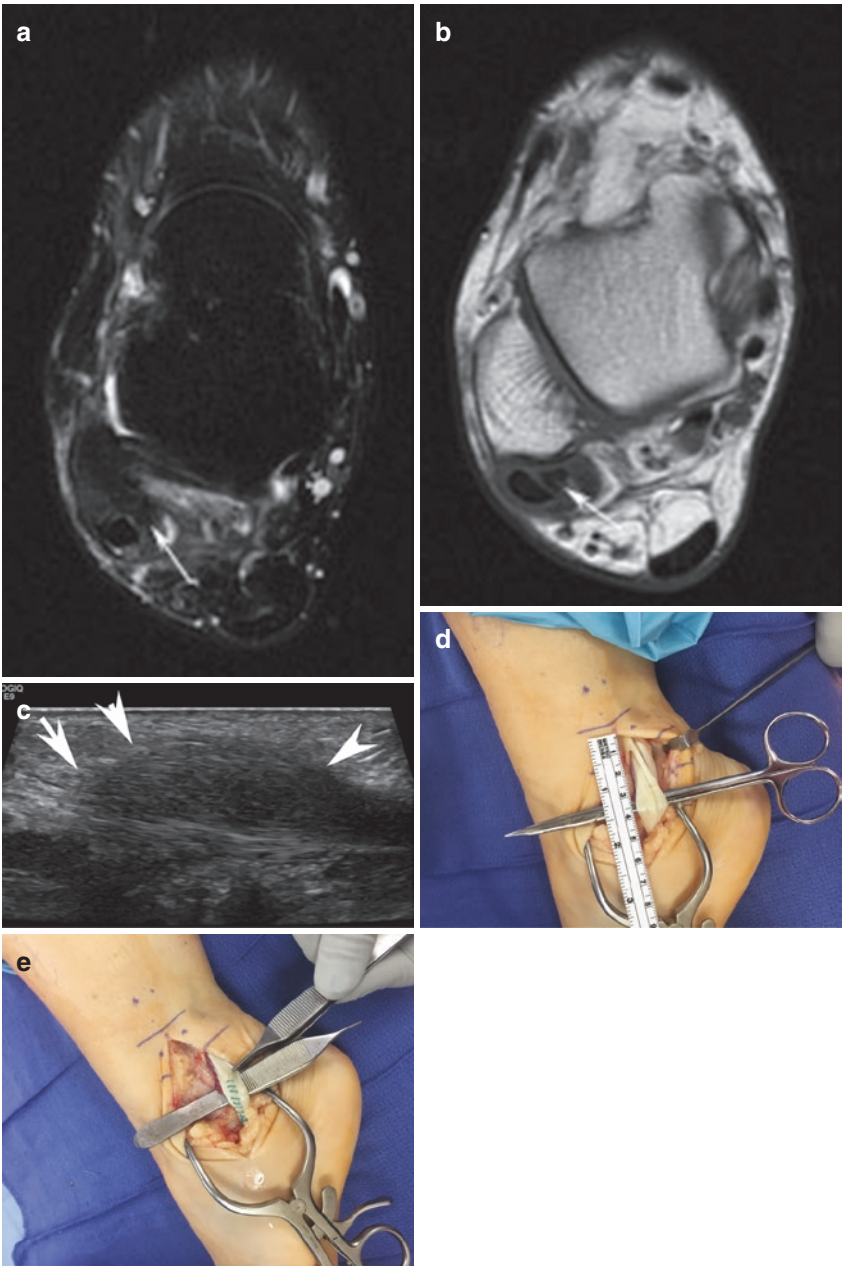

Fig. 5.8 Partial-thickness longitudinal PB tendon tear. (**a**) Axial fat-saturated T2-weighted and (**b**) axial T1-weighted MR images show an irregularity at the posterior aspect of the PB tendon with an associated intermediate- to high-signal-intensity cleft (arrow), consistent with a partial-thickness tear. (**c**) Long- axis US image shows irregularity and thickening of the PB tendon with partial loss of the normal fibrillar echotexture (arrowheads), consistent with a partial-thickness tear. (**d**) intraoperative photograph demonstrating the partial thickness tear and (**e**) following debridement of the tear and suture repair

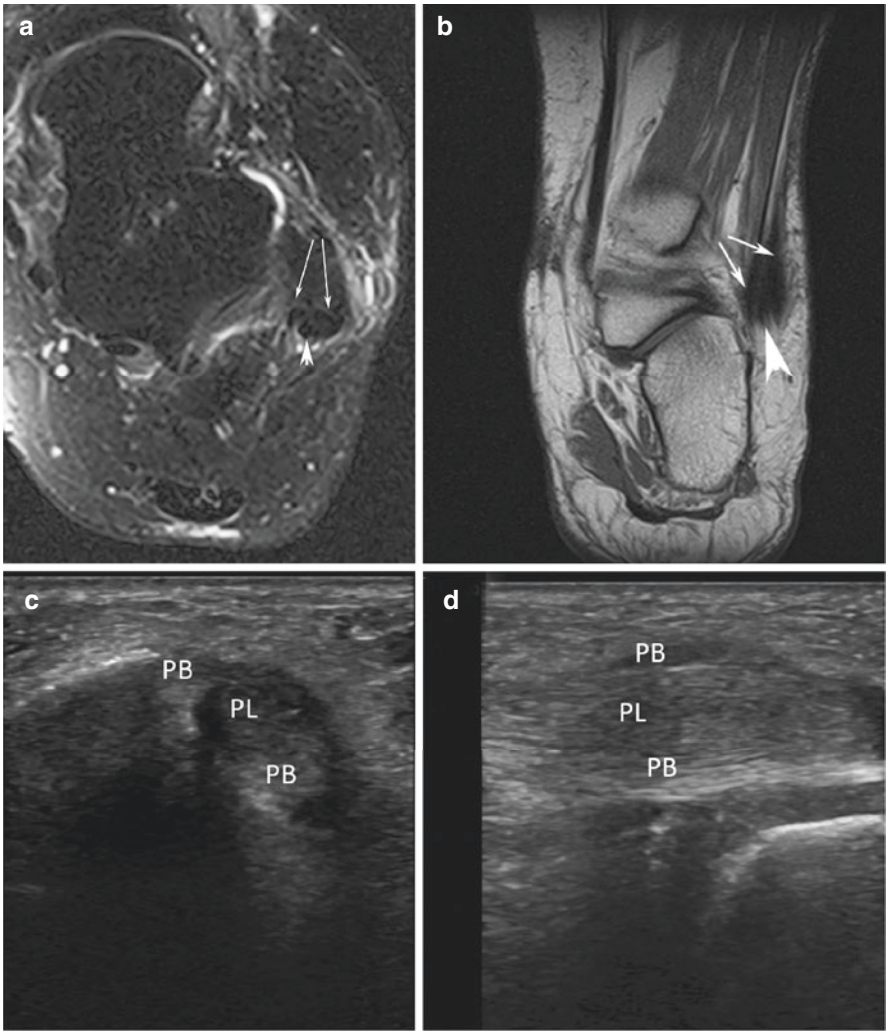

Fig. 5.9 Longitudinal split tear of PB tendon. (**a**) Axial fat-saturated T2-weighted and (**b**) coronal T1-weighted MR images show longitudinal split tear of the PB tendon at the level of retromalleolar groove with PL tendon (arrowhead) between two hemitendons of the PB (thin arrows). (**c**) Short axis and long axis (**d**) US images of the peroneal tendons at the retromalleolar groove show longitudinal split tear of the PB tendon with peroneus longus tendon between two PB hemitendons. Note heterogeneity and decreased echogenicity of the PB hemitendons and of the PL tendon consistent with pre-existing tendinosis. (**e**) Intraoperative photograph confirmed longitudinal split tear of the PB tendon

Fig. 5.9 (continued)

fortunately rare. Full-width tears or tendon ruptures show complete discontinuity of tendon fibers with variable amount of retraction (Fig. 5.10).

Peroneus longus tears are far less common than PB tears. Acute tears are more often caused by direct trauma or sporting injury. Chronic tears are commonly associated with cavovarus foot alignment [9] and hypertrophy of the peroneal tubercle [12]. PL tears can assume the same configurations as PB tears with partial and full-thickness longitudinal split tears and tendon ruptures. Longitudinal split tears commonly occur in the inframalleolar portion of the tendon in association with a hypertrophic peroneal tubercle, whereas acute tears most often occur at the cuboid tunnel where the tendon makes a 90-degree turn from the lateral to the plantar surface of the foot [9]. PL tears are often accompanied by tendinosis and tenosynovitis [20]. Other findings may include bone marrow edema in the hypertrophied peroneal tubercle and erosive changes in the cuboid [28].

Peroneal Instability

The superior peroneal retinaculum (SPR) stabilizes the peroneal tendons within the retromalleolar peroneal groove. Injury to the SPR, the fibrocartilaginous ridge (FCR) or the attachment on the SPR on the posterior fibula can lead to peroneal tendon instability (subluxation or dislocation). The initial injury often occurs with a sudden contraction of the peroneal muscles in an attempt to resist ankle inversion either during sporting activities [29, 30] or in patients with chronic ankle instability. Peroneal tendon subluxation and dislocation are common disorders with an estimated prevalence of 0.3–0.5% [31]. Factors which reduce the volume of the

retromalleolar space (including low-lying PB muscle belly, peroneus quartus, and shallow retromalleolar groove), congenital absence of SPR, and ligamentous laxity all create a predisposition to peroneal instability [12]. SPR tears are classified according to their location of the tear [30]: Grade I tears (51% of cases) involve

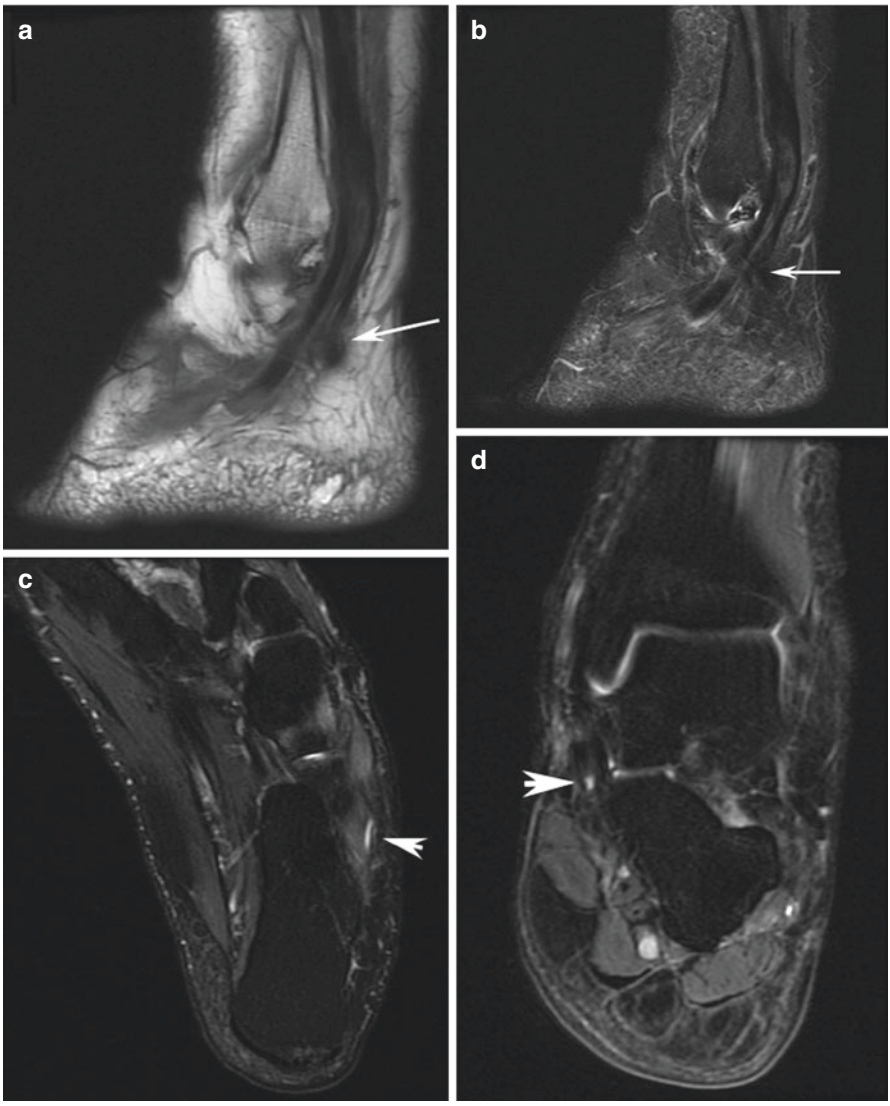

Fig. 5.10 Complete PB tendon tear with retraction. (**a**) Sagittal T1-weighted and (**b**) STIRMR images show thickening of the PB tendon. (**c**) Axial T2-weighted fat saturated and (**d**) coronal PD-weighted fat-saturated MR images show retraction of the ruptured PB tendon with fluid cleft and absence of the tendon below the lateral malleolus (arrowheads). (**e**) Intraoperative photograph confirms intact PL and completely torn PB tendons

Fig. 5.10 (continued)

stripping of the SPR from the fibula, in grade II tears (33% of cases), the FCR is elevated along with the SPR, and in grade III injuries (13% of cases), a thin fragment of bone is avulsed along with the soft tissues [32]. A grade IV injury is one in which the SPR is torn from its posterior attachment allowing the tendons to lay outside the retinaculum [30].

The ability of imaging to detect peroneal tendon instability depends on the pattern of injury. Peroneal subluxation and dislocation are not seen on plain radiographs, but can sometimes be inferred from the presence of avulsion fragment(s) at the posterior fibula which correspond to an avulsion fracture of the fibular cortex adjacent to the peroneal groove, the so-called "fleck" sign in a type III SPR tear (Fig. 5.2).

On axial MRI, the normal SPR appears as a thin low signal intensity band on all sequences. The adjacent FCR appears as a meniscus like triangular structure that is also low in signal [14]. Whereas, the injured SPR appears thickened with high signal intensity in the surrounding soft tissues on all sequences. Bone marrow edema may be present as high signal intensity seen on the fluid sensitive sequences. Peroneal subluxation or dislocation can be seen on MRI when the displacement is present at rest (Fig. 5.11). MRI is highly sensitive for fixed subluxation or dislocation of the peroneal tendons, but may miss transient subluxation and dislocation that occur only with loading and dorsiflexion of the ankle.

On US, the normal SPR appears as a thin linear hypoechoic or hyperechoic band adjacent to the peroneal tendons [7]. In contrast, the injured SPR appears thickened, irregular, and hypoechoic, and often, increased vascularity can be seen on power or color Doppler evaluation.

Fig. 5.11 Peroneal tendon subluxation, (**a**) axial T1-weighted and (**b**) T2-weighted fat saturated MR images show anterior dislocation of PL (long thin arrow) tendon, PB tendon (arrowhead) is seen in retromalleolar groove. Short axis US image shows PL tendon is anteriorly dislocated from the retromalleolar groove. Clinical images showing (**d**) anteriorly dislocated and (**e**) reduced peroneal tendons. (**f**) Intraoperative image showing dislocated peroneal tendons – note the synovialized lateral surface of the distal fibula resulting from the chronic subluxation

Fig. 5.11 (continued)

Ultrasound has the advantage of being able to be performed as a dynamic examination where the examiner can elicit symptoms or perform provocative maneuvers. In the case of peroneal subluxation or dislocation, this involves observing the position of the peroneal tendons in the fibular groove with transverse plane US during resisted dorsiflexion and eversion of the ankle [33–35] (Fig. 5.11).

Intrasheath subluxation of the peroneal tendons occurs when the SPR is intact, but the peroneal tunnel is enlarged, allowing the tendons to reverse their position behind the fibula during eversion and dorsiflexion of the hindfoot [35]. Patients who present with painful clicking but without apparent dislocation or subluxation should be evaluated with dynamic ultrasound, which demonstrates the reversal of the tendon positions.

Anatomic Variants

Os Peroneum

The os peroneum is a sesamoid bone which lies within the peroneus longus tendon at the cuboid groove. It can be either cartilaginous or ossified, ossified os peronei are found in 30% of feet [36]. It functions to enhance the moment arm of the peroneus longus [6, 7, 12]. On US it appears as a hyperechoic shadow within the PL. On MRI, an ossified os has the signal characteristics of normal bone marrow. Painful os peroneum syndrome (POPS) can occur with fracture of the os, diastasis of a multipartite os, PL tendinosis, tenosynovitis, or tendon tear (Fig. 5.12) [12, 37, 38]. The os peroneum

Fig. 5.12 Os peroneum syndrome secondary to bipartite os peroneum. Axial (**a**) T2-weighted fat saturated, (**b**) axial T1-weighted and sagittal (**c**) STIR and (**d**) T1-weighted MR images show bone marrow edema of the bipartite os peroneum consistent with clinical painful os peroneum syndrome (POPS)

Fig. 5.13 Os peroneum fracture. (**a**) Lateral and (**b**) oblique radiographs show a fractured os peroneum (arrows) with a more than 6-mm distraction of the fracture fragments about the calcaneocuboid joint, a finding indicative of a PL tendon tear. (**c**) Coronal T1-weighted and (**d**) PD-weighted fat saturated MR images show fractured os peroneum (arrowhead) with associated PL tendon rupture

can be displaced in peroneus longus tears (displaced distally in proximal tears, and displaced proximally in distal tears). The displaced os peroneum in PL tendon tear or the displaced fragments in os peroneum fracture can be seen on XR (Fig. 5.13a and b).

Peroneus Quartus

The peroneus quartus is an accessory muscle that is present in 12–22% of individuals [39, 40]. It normally originates from the peroneus brevis. It most commonly

inserts into a hypertrophied peroneal tubercle on the calcaneus, though it can also insert on other locations on the calcaneus, the PL, the PB, or the fifth metatarsal. It does not have a defined function. It occupies space within the peroneal groove and its presence is associated with a doubling of the risk of peroneal tendonitis and peroneal tendon tears [25]. On MRI, the peroneus quartus muscle shows intermediate signal intensity and its tendon shows low signal intensity on all sequences. On US, the peroneus quartus muscle belly appears hypoechoic with respect to its hyperechoic tendon [41] (Fig. 5.14).

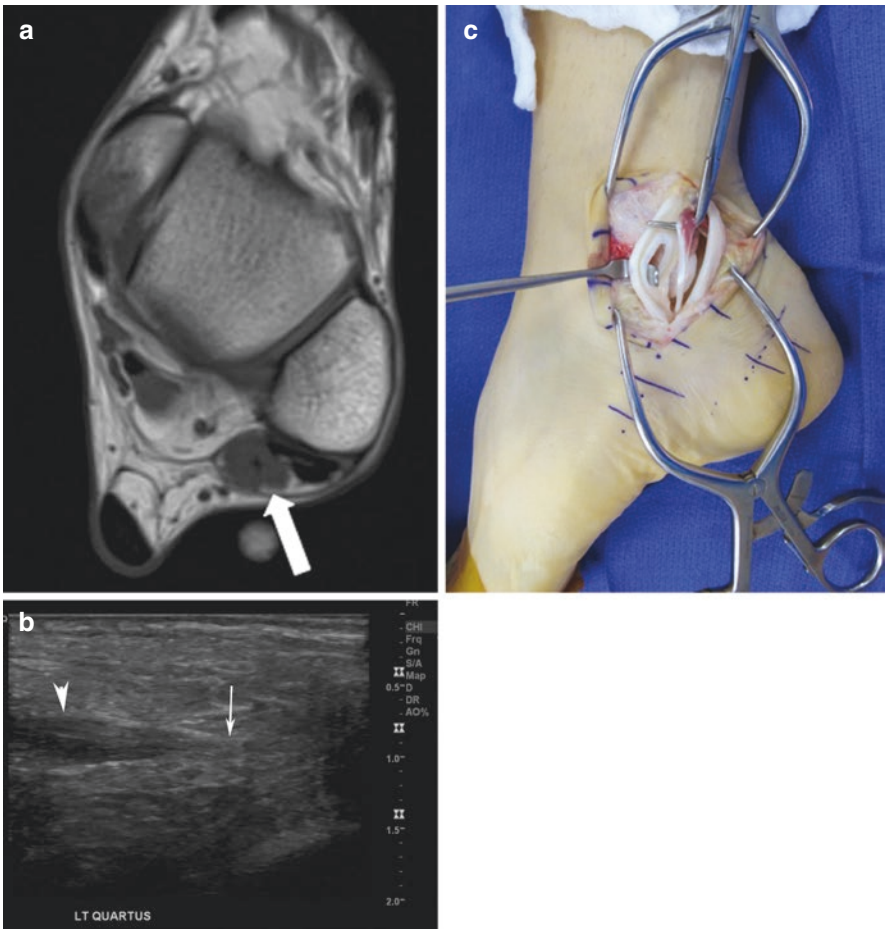

Fig. 5.14 Peroneus quartus muscle. (**a**) Axial T1-weighted MR image shows a small peroneus quartus muscle (white block arrow) posterior to PL and PB tendons causing crowding in the retromalleolar groove. (**b**) Long axis US image at the lateral malleolus shows a hypoechoic peroneus quartus muscle (arrowhead) with hyperechoic tendon (arrows) coursing distally. (**c**) Intraoperative image showing peroneus quartus muscle and tendon lying posterior to longitudinally split PB tendon

Low-Lying Peroneus Brevis Muscle Belly

The muscle belly of the peroneus brevis extends more distally than that of the peroneus longus. The distance between the PB muscle belly and the tip of the fibula is highly variable and depends on the angle of ankle flexion at the time of measurement. There is a lack of consensus as to how far distal the muscle belly normally extends. A number of studies have found the distal extent of the muscle belly occurring somewhere between 27 mm proximal to and 13 mm distal to the tip of the fibula with a median of 0 mm in normal individuals [19]. Thus, it is generally accepted that a muscle belly that extends more than 15 mm below the tip of the fibula is considered "low lying" [19]. The low-lying PB muscle belly can cause congestion within the peroneal groove and is associated with peroneal tendonitis and peroneal tendon tears [37, 42, 43] (Fig. 5.15).

A retrospective review of patients surgically treated for peroneal tendon symptoms found a lower lying muscle belly in patients with surgically confirmed tears (30.3 ± 9 mm above the tip) compared to those without tears(38.4 ± 8 mm above) and those without peroneal tendon symptoms(46.3 ± 11 mm) [44].

Hypertrophic Protuberances of the Lateral Calcaneus

The retrotrochlear eminence is a bony prominence located posterior to the peroneal tendons and is present in 98% of calcanei [12]. Hypertrophy is associated with the presence of a PQ. The peroneal tubercle is a bony prominence, which serves as the attachment site for the IPR and functions to provide a fulcrum for the PL as its course diverges from that of the PB. It is present in 90% of calcanei [45]. It is considered to be enlarged when it projects more than 5 mm past the lateral wall of the calcaneus (Fig. 5.16). A little over one-quarter of peroneal tubercles are enlarged with a concave shape [45]. The hypertrophied peroneal tubercle can irritate the PL or its sheath leading to tenosynovitis, partial or complete tendon tear, or bursitis [12, 23, 45].

Peroneal Groove Shape

The retromalleolar peroneal groove is variable in shape. The shape of the groove is best assessed on axial MR images taken 1 cm proximal to the level of the plafond. The groove is determined to have a concave shape when the posterior fibular surface has an anteriorly directed depression, a flat shape when there is no depression, and a convex shape when the central portion of the posterior cortex bulges posteriorly [46]. A concave fibular groove is found in 68% of cadaveric fibulae and a flat or convex groove in 32% [47]. The flat and convex groove are thought to be associated with an increased risk of peroneal tendon instability. However, the association of fibular groove shape with risk of dislocation has recently become the subject of

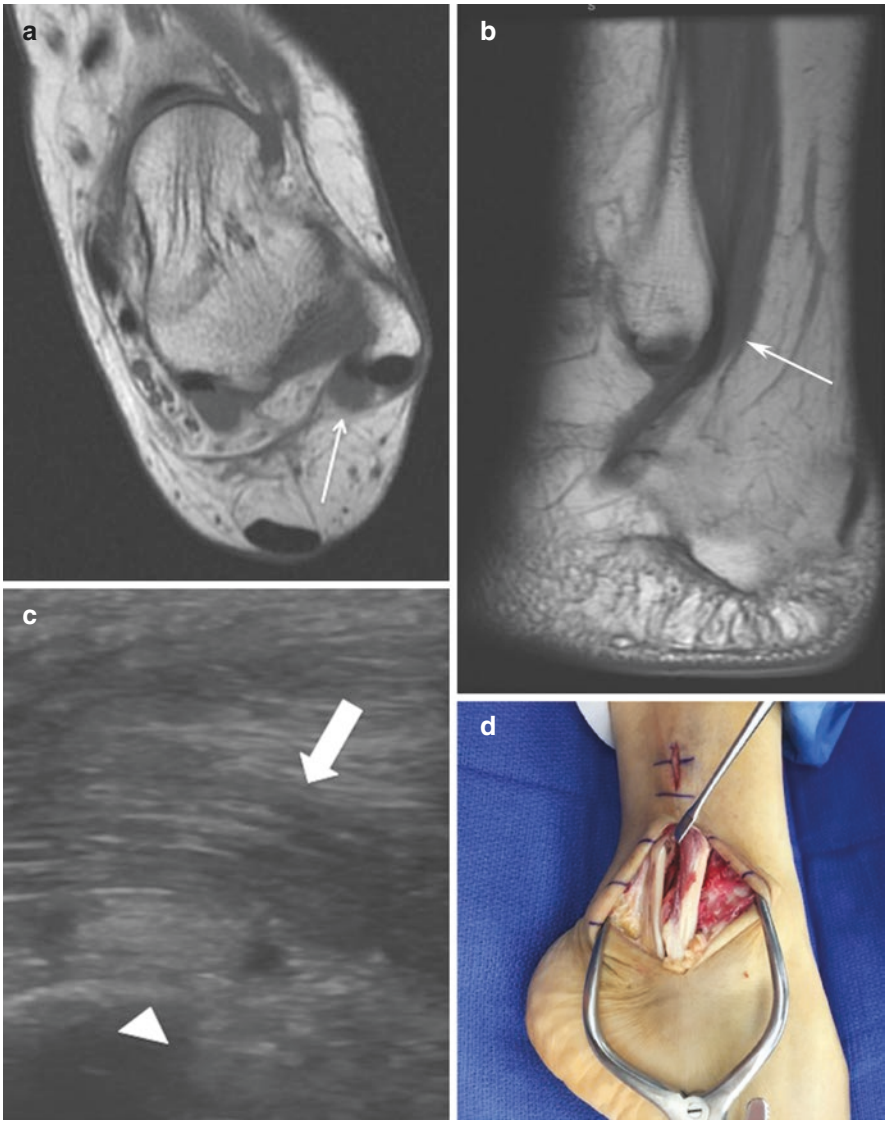

Fig. 5.15 Low-lying PB muscle belly. (**a**) Axial and (**b**) sagittal T1-weighted MR images show low-lying PB muscle belly (white thin arrows) extending below the lateral malleolus. (**c**) Long axis US image shows low-lying PB muscle belly (block arrow) extending below the lateral malleolus (white arrowhead). (**d**) Intraoperative image showing low-lying PB muscle belly

controversy, as recent studies have found no differences in morphology between patients with and without instability instead focusing on the fibrocartilaginous ridge as the primary stabilizer of the tendons [48].

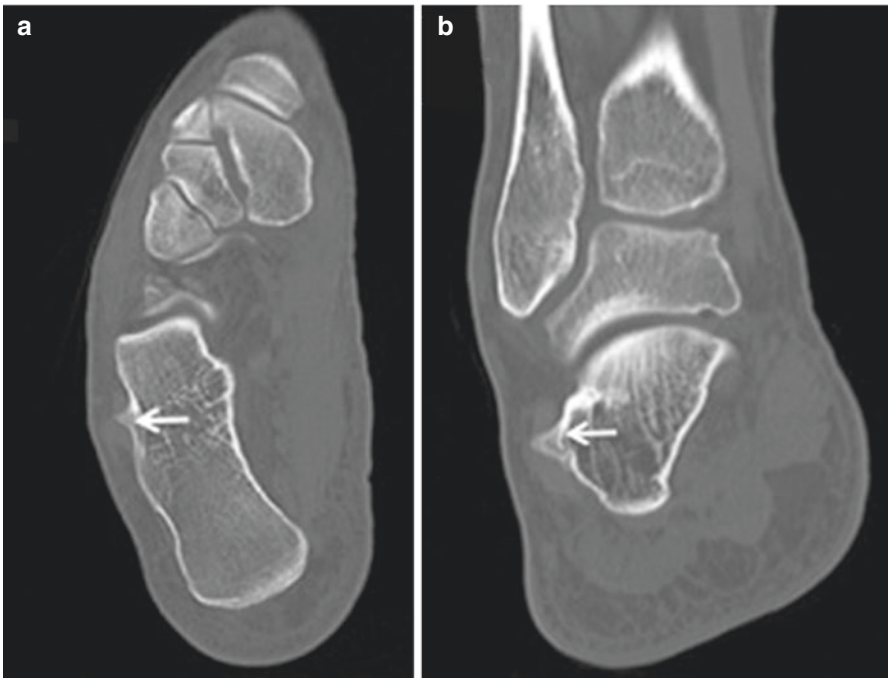

Fig. 5.16 (**a**) Axial and (**b**) coronal reformatted CT images show enlarged peroneal tubercle (arrow)

Summary

Imaging of patients with suspected peroneal tendon disorders should include weight-bearing radiographs of the ankle and foot, as they are useful for the detection of avulsion fractures, the presence of an os peroneum, and for the evaluation of cavovarus alignment. Advance imaging in the form of MRI or ultrasound imaging is often needed to differentiate between peroneal tendonitis (tendinosis and/or tenosynovitis), tears, and subluxation. MRI has the advantages of supplying information about a wide array of related and concomitant conditions and being useful for preoperative planning. In contrast, US is a less time-consuming and a less costly examination, which provides equivalent diagnostic accuracy for tears and is superior in the detection of tendon subluxation. Both modalities are capable of providing information about the presence the anatomic variants, including low-lying peroneus brevis muscle belly, os peroneum, peroneus quartus, and hypertrophied peroneal tubercle.

References

1. Lamm BM, Myers DT, Dombek M, Mendicino RW, Catanzariti AR, Saltrick K. Magnetic resonance imaging and surgical correlation of peroneus brevis tears. J Foot Ankle Surg. 2004;43(1):30–6. https://doi.org/10.1053/j.jfas.2003.11.002.
2. Khoury NJ, el-Khoury GY, Saltzman CL, Kathol MH. Peroneus longus and brevis tendon tears: MR imaging evaluation. Radiology. 1996;200(3):833–41.
3. Park HJ, Lee SY, Park NH, Rho MH, Chung EC, Kwag HJ. Accuracy of MR findings in characterizing peroneal tendons disorders in comparison with surgery. Acta Radiol. 2012;53(7):795–801. https://doi.org/10.1258/ar.2012.120184.
4. Waitches GM, Rockett M, Brage M, Sudakoff G. Ultrasonographic-surgical correlation of ankle tendon tears. J Ultrasound Med. 1998;17(4):249–56.
5. Grant TH, Kelikian AS, Jereb SE, McCarthy RJ. Ultrasound diagnosis of peroneal tendon tears. A surgical correlation. J Bone Joint Surg Am. 2005;87(8):1788–94. https://doi.org/10.2106/JBJS.D.02450.
6. Lee SJ, Jacobson JA, Kim SM, et al. Ultrasound and MRI of the peroneal tendons and associated pathology. Skelet Radiol. 2013;42(9):1191–200. https://doi.org/10.1007/s00256-013-1631-6.
7. Bianchi S, Delmi M, Molini L. Ultrasound of peroneal tendons. Semin Musculoskelet Radiol. 2010;14(3):292–306. https://doi.org/10.1055/s-0030-1254519.
8. Klauser AS, Peetrons P. Developments in musculoskeletal ultrasound and clinical applications. Skelet Radiol. 2010;39(11):1061–71. https://doi.org/10.1007/s00256-009-0782-y.
9. Brandes CB, Smith RW. Characterization of patients with primary peroneus longus tendinopathy: a review of twenty-two cases. Foot Ankle Int. 2000;21(6):462–8. https://doi.org/10.1177/107110070002100602.
10. Saltzman CL, el-Khoury GY. The hindfoot alignment view. [see comment]. Foot Ankle Int. 1995;16(9):572–6.
11. Schubert R. MRI of peroneal tendinopathies resulting from trauma or overuse. Br J Radiol. 2013;86(1021):20110750. https://doi.org/10.1259/bjr.20110750.
12. Wang XT, Rosenberg ZS, Mechlin MB, Schweitzer ME. Normal variants and diseases of the peroneal tendons and superior peroneal retinaculum: MR imaging features. Radiographics. 2005;25(3):587–602. https://doi.org/10.1148/rg.253045123.
13. Mengiardi B, Pfirrmann CW, Schottle PB, et al. Magic angle effect in MR imaging of ankle tendons: influence of foot positioning on prevalence and site in asymptomatic subjects and cadaveric tendons. Eur Radiol. 2006;16(10):2197–206. https://doi.org/10.1007/s00330-006-0164-y.
14. Demondion X, Canella C, Moraux A, Cohen M, Bry R, Cotten A. Retinacular disorders of the ankle and foot. Semin Musculoskelet Radiol. 2010;14(3):281–91. https://doi.org/10.1055/s-0030-1254518.
15. Taljanovic MS, Gimber LH, Becker GW, et al. Shear-wave elastography: basic physics and musculoskeletal applications. Radiographics. 2017;37(3):855–70. https://doi.org/10.1148/rg.2017160116.
16. Taljanovic MS, Melville DM, Klauser AS, et al. Advances in lower extremity ultrasound. Curr Radiol Rep. 2015;3(6):1–12.
17. DiGiovanni BF, Fraga CJ, Cohen BE, Shereff MJ. Associated injuries found in chronic lateral ankle instability. Foot Ankle Int. 2000;21(10):809–15.
18. Kijowski R, De Smet A, Mukharjee R. Magnetic resonance imaging findings in patients with peroneal tendinopathy and peroneal tenosynovitis. Skelet Radiol. 2007;36(2):105–14. https://doi.org/10.1007/s00256-006-0172-7.
19. Saupe N, Mengiardi B, Pfirrmann CW, Vienne P, Seifert B, Zanetti M. Anatomic variants associated with peroneal tendon disorders: MR imaging findings in volunteers with asymptomatic ankles. Radiology. 2007;242(2):509–17. https://doi.org/10.1148/radiol.2422051993.
20. Wang CC, Wang SJ, Lien SB, Lin LC. A new peroneal tendon rerouting method to treat recurrent dislocation of peroneal tendons. Am J Sports Med. 2009;37(3):552–7. https://doi.org/10.1177/0363546508325924.

21. Bencardino JT, Rosenberg ZS, Serrano LF. MR imaging features of diseases of the peroneal tendons. Magn Reson Imaging Clin N Am. 2001;9(3):493–505, x.
22. Mota J, Rosenberg ZS. Magnetic resonance imaging of the peroneal tendons. Top Magn Reson Imaging. 1998;9(5):273–85.
23. Bruce WD, Christofersen MR, Phillips DL. Stenosing tenosynovitis and impingement of the peroneal tendons associated with hypertrophy of the peroneal tubercle. Foot Ankle Int. 1999;20(7):464–7. https://doi.org/10.1177/107110079902000713.
24. Taki K, Yamazaki S, Majima T, Ohura H, Minami A. Bilateral stenosing tenosynovitis of the peroneus longus tendon associated with hypertrophied peroneal tubercle in a junior soccer player: a case report. Foot Ankle Int. 2007;28(1):129–32. https://doi.org/10.3113/FAI.2007.0022.
25. Sobel M, Bohne WH, Levy ME. Longitudinal attrition of the peroneus brevis tendon in the fibular groove: an anatomic study. Foot Ankle. 1990;11(3):124–8.
26. Squires N, Myerson MS, Gamba C. Surgical treatment of peroneal tendon tears. Foot Ankle Clin. 2007;12(4):675–95, vii. https://doi.org/10.1016/j.fcl.2007.08.002.
27. Sobel M, Geppert MJ, Olson EJ, Bohne WH, Arnoczky SP. The dynamics of peroneus brevis tendon splits: a proposed mechanism, technique of diagnosis, and classification of injury. Foot Ankle. 1992;13(7):413–22.
28. O'Donnell P, Saifuddin A. Cuboid oedema due to peroneus longus tendinopathy: a report of four cases. Skelet Radiol. 2005;34(7):381–8. https://doi.org/10.1007/s00256-005-0907-x.
29. Butler BW, Lanthier J, Wertheimer SJ. Subluxing peroneals: a review of the literature and case report. J Foot Ankle Surg. 1993;32(2):134–9.
30. Oden RR. Tendon injuries about the ankle resulting from skiing. Clin Orthop Relat Res. 1987;216:63–9.
31. Magnano GM, Occhi M, Di Stadio M, Toma P, Derchi LE. High-resolution US of non-traumatic recurrent dislocation of the peroneal tendons: a case report. Pediatr Radiol. 1998;28(6):476–7. https://doi.org/10.1007/s002470050388.
32. Eckert WR, Davis EA Jr. Acute rupture of the peroneal retinaculum. J Bone Joint Surg Am. 1976;58(5):670–2.
33. Neustadter J, Raikin SM, Nazarian LN. Dynamic sonographic evaluation of peroneal tendon subluxation. AJR Am J Roentgenol. 2004;183(4):985–8. https://doi.org/10.2214/ajr.183.4.1830985.
34. Raikin SM. Intrasheath subluxation of the peroneal tendons. Surgical technique. J Bone Joint Surg Am. 2009;91(Suppl 2 Pt 1):146–55. https://doi.org/10.2106/jbjs.h.01356.
35. Raikin SM, Elias I, Nazarian LN. Intrasheath subluxation of the peroneal tendons. J Bone Joint Surg Am. 2008;90(5):992–9. https://doi.org/10.2106/jbjs.g.00801.
36. Muehleman C, Williams J, Bareither ML. A radiologic and histologic study of the os peroneum: prevalence, morphology, and relationship to degenerative joint disease of the foot and ankle in a cadaveric sample. Clin Anat. 2009;22(6):747–54. https://doi.org/10.1002/ca.20830.
37. Bashir WA, Lewis S, Cullen N, Connell DA. Os peroneum friction syndrome complicated by sesamoid fatigue fracture: a new radiological diagnosis? Case report and literature review. Skelet Radiol. 2009;38(2):181–6. https://doi.org/10.1007/s00256-008-0588-3.
38. Sobel M, Pavlov H, Geppert MJ, Thompson FM, DiCarlo EF, Davis WH. Painful os peroneum syndrome: a spectrum of conditions responsible for plantar lateral foot pain. Foot Ankle Int. 1994;15(3):112–24. https://doi.org/10.1177/107110079401500306.
39. Cheung YY, Rosenberg ZS, Ramsinghani R, Beltran J, Jahss MH. Peroneus quartus muscle: MR imaging features. Radiology. 1997;202(3):745–50. https://doi.org/10.1148/radiology.202.3.9051029.
40. Sobel M, Levy ME, Bohne WH. Congenital variations of the peroneus quartus muscle: an anatomic study. Foot Ankle. 1990;11(2):81–9.
41. Griffith, James F. An introduction to musculoskeletal ultraound. In. Rotations in Radiology-Musculoskeletal Imaging Volume 2 Metabolic, Infectious, and Congenital Diseases; Internal Derangement of the Joints; and Arthrography and Ultrasound In: Mihra ST, Imran MO, Kevin BH, and Tyson SC, editors. Musculoskeletal imaging, rotations in radiology. New York:

Oxford University Press; 2019. p. 329–40. https://global.oup.com/academic/product/musculoskeletal-imaging-volume-2-9780190938178?lang=en&cc=us#.
42. Geller J, Lin S, Cordas D, Vieira P. Relationship of a low-lying muscle belly to tears of the peroneus brevis tendon. Am J Orthop (Belle Mead NJ). 2003;32(11):541–4.
43. Mirmiran R, Squire C, Wassell D. Prevalence and role of a low-lying peroneus brevis muscle belly in patients with peroneal tendon pathologic features: a potential source of tendon subluxation. J Foot Ankle Surg. 2015;54(5):872–5. https://doi.org/10.1053/j.jfas.2015.02.012.
44. Freccero DM, Berkowitz MJ. The relationship between tears of the peroneus brevis tendon and the distal extent of its muscle belly: an MRI study. Foot Ankle Int. 2006;27(4):236–9.
45. Hyer CF, Dawson JM, Philbin TM, Berlet GC, Lee TH. The peroneal tubercle: description, classification, and relevance to peroneus longus tendon pathology. Foot Ankle Int. 2005;26(11):947–50.
46. Rosenberg ZS, Bencardino J, Astion D, Schweitzer ME, Rokito A, Sheskier S. MRI features of chronic injuries of the superior peroneal retinaculum. AJR Am J Roentgenol. 2003;181(6):1551–7. https://doi.org/10.2214/ajr.181.6.1811551.
47. Ozbag D, Gumusalan Y, Uzel M, Cetinus E. Morphometrical features of the human malleolar groove. Foot Ankle Int. 2008;29(1):77–81. https://doi.org/10.3113/fai.2008.0077.
48. Adachi N, Fukuhara K, Kobayashi T, Nakasa T, Ochi M. Morphologic variations of the fibular malleolar groove with recurrent dislocation of the peroneal tendons. Foot Ankle Int. 2009;30(6):540–4. https://doi.org/10.3113/fai.2009.0540.